

# Luminal Loop M672-P707 of the Menkes Protein (ATP7A) Transfers Copper to Peptidylglycine Monooxygenase

Adenike Otoikhian,<sup>†</sup> Amanda N. Barry,<sup>‡,§</sup> Mary Mayfield,<sup>†</sup> Mark Nilges,<sup>§</sup> Yiping Huang,<sup>‡</sup> Svetlana Lutsenko,<sup>‡</sup> and Ninian J. Blackburn<sup>\*,†</sup>

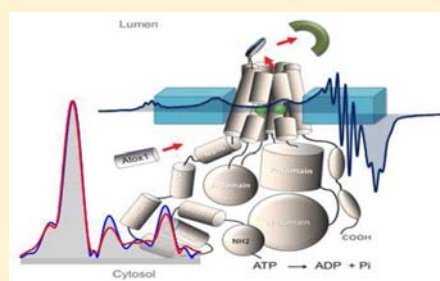
<sup>†</sup>Institute of Environmental Health, Oregon Health & Sciences University, Beaverton, Oregon 97006, United States

<sup>‡</sup>Department of Physiology, The Johns Hopkins University, Baltimore, Maryland 21205, United States

<sup>§</sup>Illinois EPR Research Center, Urbana, Illinois 61801, United States

## Supporting Information

**ABSTRACT:** Copper transfer to cuproproteins located in vesicular compartments of the secretory pathway depends on activity of the copper-translocating ATPase (ATP7A), but the mechanism of transfer is largely unexplored. Copper-ATPase ATP7A is unique in having a sequence rich in histidine and methionine residues located on the luminal side of the membrane. The corresponding fragment binds Cu(I) when expressed as a chimera with a scaffold protein, and mutations or deletions of His and/or Met residues in its sequence inhibit dephosphorylation of the ATPase, a catalytic step associated with copper release. Here we present evidence for a potential role of this luminal region of ATP7A in copper transfer to cuproenzymes. Both Cu(II) and Cu(I) forms were investigated since the form in which copper is transferred to acceptor proteins is currently unknown. Analysis of Cu(II) using EPR demonstrated that at Cu:P ratios below 1:1 <sup>15</sup>N-substituted protein had Cu(II) bound by 4 His residues, but this coordination changed as the Cu(II) to protein ratio increased toward 2:1. XAS confirmed this coordination via analysis of the intensity of outer-shell scattering from imidazole residues. The Cu(II) complexes could be reduced to their Cu(I) counterparts by ascorbate, but here again, as shown by EXAFS and XANES spectroscopy, the coordination was dependent on copper loading. At low copper Cu(I) was bound by a mixed ligand set of His + Met, whereas at higher ratios His coordination predominated. The copper-loaded loop was able to transfer either Cu(II) or Cu(I) to peptidylglycine monooxygenase in the presence of chelating resin, generating catalytically active enzyme in a process that appeared to involve direct interaction between the two partners. The variation of coordination with copper loading suggests copper-dependent conformational change which in turn could act as a signal for regulating copper release by the ATPase pump.



## INTRODUCTION

Mammalian cuproenzymes such as peptidylglycine  $\alpha$ -amidating monooxygenase (PAM),<sup>1</sup> dopamine  $\beta$ -monooxygenase (DBM),<sup>2</sup> tyrosinase,<sup>3</sup> and extracellular superoxide dismutase (SOD3)<sup>4</sup> mature within vesicles of the secretory pathway. These enzymes contain copper centers, which cycle between the Cu(I) and Cu(II) states during catalysis. PAM catalyzes the C-terminal amidation of glycine-extended neuropeptides, while DBM catalyzes the benzylic hydroxylation of dopamine to norepinephrine. Their catalytic cores contain two mononuclear copper centers (CuH and CuM), with CuH coordinated by three histidine residues and CuM coordinated by two histidines and a methionine.<sup>5–8</sup> Tyrosinase contains a coupled binuclear copper center with each Cu coordinated to three histidines<sup>9</sup> and catalyzes the hydroxylation of catechols to quinones ultimately forming the pigment melanin. SOD3 contains an active site similar to the Cu-Zn containing SOD1 family, with a mononuclear Cu center coordinated by four histidines one of which bridges to the Zn atom and is found in significant amounts in endothelial cells, where it performs a protective role against the effects of excess superoxide.<sup>10</sup>

Although the mechanism of copper insertion into these proteins is largely unexplored, an increasing amount of data points to a key role for copper-transporting ATPases.<sup>10–13</sup> These are members of the P1B family of heavy metal transporters and are found in all forms of life from bacteria to mammals where they function in copper export across membranes. The proteins have a multidomain structure with an N-terminal regulatory domain, a cytosolic ATP binding domain, and a transmembrane domain that is usually comprised of eight transmembrane helices.<sup>14</sup> The bacterial CopA from *Legionella pneumophila*<sup>15</sup> is currently the only copper-transporting ATPase for which a crystal structure is available and provides a template for understanding the transport mechanism. However, the mammalian homologues ATP7A and 7B differ from CopA in the presence of a more complex N-terminal regulatory domain comprised of six metal binding subdomains, each of which binds Cu(I), and a small domain between TMs 1 and 2 that extends outward from the luminal

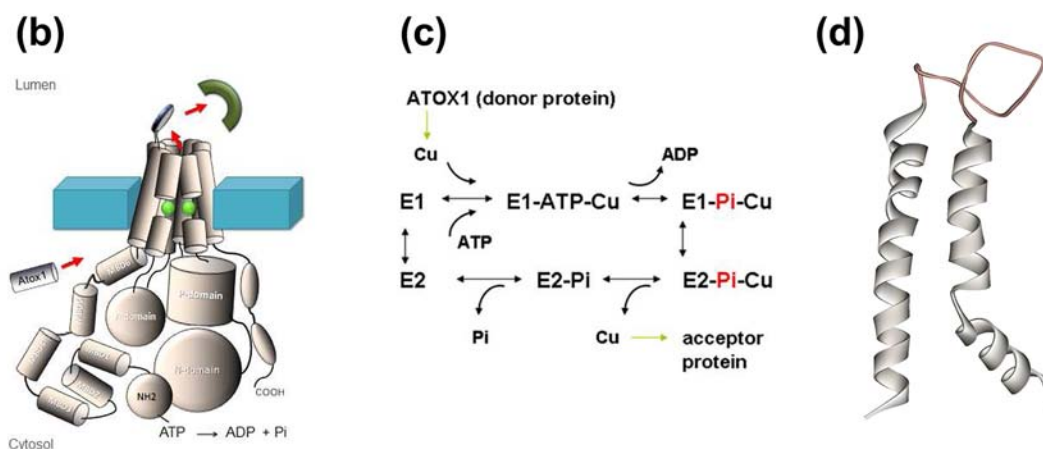
Received: February 6, 2012

Published: May 13, 2012

Scheme 1<sup>a</sup>

(a)

MGLMIYMMVDHHLATLHHNQNSKEEMINLHSSMFLERQILPGLSVMNLLSFLI human  
 MGLMVYMMVDHHLATLHHNQNSNEEMINMHSAMFLERQILPGLSIMNLLSLLL mouse  
 MGLMIYMMVDHHLATLHHNQNSNEEMINMHSAMFLERQILPGLSIMNLLSLLL rat  
 MGLMIYMMVDHHLATLHHNQNSQEEMINSHSSMFLERQILPGLSIMNLLSFLI pig  
 MGLMIYMMVDHHLAAILHHNQNSQEEMINIHSAMFLERQILPGLSIMNLLSFLI dog  
 MGLMIYMMVDHHLASLQHNSQEEMINIHSAMFLERQILPGLSIMNLLSFLI cow  
 MGLMIYMMVDHHLLETLHHNQNSQEEMIHHSAMFLERQILPGLSIMNLLSFLI horse  
 MGLMIYMMVDHHLATLHHNQNSNEEMINIHSAMFLERQIMPGLSIMNLLSFLI rabbit  
 MGLMIYMMVMDRYLAALHHNQNTMSQEEMINIHSAMFLEHQILPGLSIMNLLSFLI elephant  
 MAMMIYMMVVDSDLSDAHRHLNMSSEEMEAIHSAMFLEHQLLPGLSVMNFLSFLI turkey  
 MGGMIYMIIVVDHMDIKYHQHNNATAEDRAKYHSTMFLEKQLLPGLSIMNLLSFLI zebrafish  
 MGLMMYMMAMEHHLATLHHNQNSNEEMIKIHSAMFLERQILPGLSIMNLLSLLL hamster  
 MGGHG-----LKHFISSNGSSWIQLLLATP CopA



<sup>a</sup>(a) Sequence comparisons of the luminal loop region of ATP7A from different organisms with the end of TM1 and start of TM2 shaded in the first sequence. (b) Cartoon of the domain structure of PIB type ATPases. (c) Catalytic mechanism for PIB type ATPases. (d) Modeled structure of TM helices 1 and 2 of ATP7B showing the location of the luminal loop. (Note that this modeled structure does not contain the more extended loop found in ATP7A). Model based on that developed in Schushan, M.; Bhattarjee, A.; Ben-Tal, N.; Lutsenko, S. A structural model of the copper ATPase ATP7B: interpretation of Wilson disease-causing mutations and details of the transport mechanism. *Metallomics* 2012 (submitted).

side of the membrane (Scheme 1). Cuproprotein loading is a catalytic process beginning with a high affinity conformer of the ATPase, E1, with copper bound at a transmembrane site. This activates ATP-dependent phosphorylation of the protein, which in turn drives a conformational change leading to the occlusion of copper from the cytosolic side. Copper release on the luminal side is accompanied by dephosphorylation and the generation of the low affinity E2 form, ready to rebind copper and restart the catalytic cycle.<sup>16,17</sup>

Whereas cytosolic cuproproteins are metalated via copper chaperones,<sup>18–20</sup> existing evidence suggests that copper delivery within the lumen of secretory granules may not rely on specific chaperones,<sup>21</sup> rather that ATP7A is able to transfer copper directly to vesicular cuproenzymes with different structures and copper coordination. Additionally, since the cuproenzyme targets are redox active and cycle between Cu(I) and Cu(II), the oxidation state required for copper loading is unknown. While it is possible that a specific chaperone for vesicular copper transport may yet be discovered, we have put forward an alternative hypothesis that the luminal loop between transmembrane segments 1 and 2 acts as an important sensor for acceptor protein loading and may be involved in direct ATPase-acceptor interactions.<sup>16</sup> As shown in Scheme 1a

this loop is rich in Met and His residues. Met-rich domains are ubiquitous in copper-transport proteins and often signal areas of the protein involved in Cu(I) binding or selectivity,<sup>22–25</sup> whereas His-rich domains often bind Cu(II). We have therefore proposed that the luminal loop in ATP7A binds copper as it exits the membrane and selectively hands it off to apo-cuproproteins either as Cu(I) or as Cu(II) formed by redox chemistry at the luminal copper binding sites.

In support of our hypothesis we recently showed that mutations of His and/or Met residues within the luminal loop of ATP7A had a major effect on the rate of dephosphorylation and thus directly affect the catalytic step involving copper release into the luminal space.<sup>26</sup> Investigation of copper binding to the luminal loop of full-length ATP7A is complicated by Cu(I) binding to the N-terminal and intramembrane domains, making it difficult to separate binding events in the luminal loop from those elsewhere in the protein. Therefore we prepared a “model system” in which the luminal peptide was inserted as a loop of sequence within a small soluble protein scaffold, which itself contained no metal binding Cys, Met, or His residues and demonstrated the ability of the insert to bind copper.<sup>26</sup> In the present paper, we more accurately define the Cu(I) and Cu(II) binding sites using XAS

and EPR spectroscopy and show that the metal loaded chimera transfers copper to the apo form of the catalytic core of the monooxygenase domain of PAM (hereafter termed apo-PHM) in a facile manner.

## MATERIALS AND METHODS

All buffers used were reagent grade, purchased from Sigma-Aldrich at a minimum purity of 99%. Sodium ascorbate, copper(II) sulfate pentahydrate, and tetrakis(acetonitrile)copper(I) hexafluorophosphate were also purchased from Sigma-Aldrich. Beef liver catalase was from Roche. The enzyme substrate, dansyl-Tyr-Val-Gly (dansyl-YVG), was obtained from American Peptide Co. The copper chelating agent, Chelex-100 resin (100–200 mesh, sodium form), was obtained from Bio-Rad Laboratories. The resin was cleaned by soaking overnight in 5 M HCl, equilibrated with 50 mM sodium phosphate buffer at pH 8.0, and air-dried. Distilled deionized water used throughout the experiments was purified to a resistivity of 17–18 M $\Omega$  with a Barnstead Nanopure II system.

**Construction of ScoHM Chimera.** The chimeric protein, ScoHM, was constructed by replacing the C<sup>45</sup>XXXC<sup>49</sup> copper binding motif of a Met52/Met56Ile-His55/His135A quadruple mutant of *Bacillus subtilis* Sco (BSco)<sup>27</sup> protein with the luminal loop Histidine-Methionine (HM) rich peptide (MDHFFATLHHNQNSKEE-MINLHSSM) of the Menkes protein (ATP7A) as previously described.

**Preparation of Strep-tag II/ScoHM/pTXB-3 Fusion Protein.** Strep-tag II/ScoHM fusion protein was constructed by polymerase chain reaction amplification of ScoHM plasmid to include a Strep-tag II affinity tag (pASK-IBA5, Genosys Biotechnologies Inc.) at the N-terminus of ScoHM by using the primers 5'-TATTACCATGGCTAGCGCTTGGAGCCACCGCATTCGAAAA-GACACACATAAA GACAGCAGATTAAAGATCCG-3' (strep-tag underlined), and the MXE intein reverse primer. The forward primer introduced a new NcoI site containing an ATG start codon followed by the strep-tag II, thus eliminating the original NcoI site in ScoHM. The MXE intein reverse primer located in pTXB3 expression vector (New England BioLabs) includes a unique SpeI site. The polymerase chain reaction product containing the Strep-tag II affinity tag, the complete ScoHM, and a small portion of pTXB-3 with a unique SpeI site was digested with NcoI SpeI and cloned into NcoI SpeI sites in pTXB-3. The pTXB-3 expression vector allows for a translational fusion of an MxeGyrA intein tag to the C-terminus of the Strep-tag II/ScoHM fusion protein. The validity of construct was checked by DNA sequencing. The ligation mixture of the Strep-tag II/ScoHM/pTXB-3 fusion protein was termed 5'-Stag ScoHM.

**Expression and Purification of ScoHM and Its 5'-Stag ScoHM Variant.** ScoHM plasmid and 5'-Stag ScoHM were transformed, separately, into the *Escherichia coli* strain ER2566 (New England BioLabs). Protein expression and purification were carried out using protocols described previously.<sup>27</sup> Briefly, cells expressing the soluble proteins were grown in 1 L of LB-glucose medium containing 100  $\mu$ g/mL of ampicillin at 37 °C to a final A<sub>600</sub> between 0.6 and 0.9. Protein expression was induced by adding 500  $\mu$ M isopropyl- $\beta$ -thiogalactopyranoside (IPTG) at 17 °C with shaking for 20 h. The cells were harvested by centrifugation in a Sorvall GS-3 rotor at 8000g for 30 min and frozen at -80 °C (as needed). Apoproteins were purified from the soluble lysate by resuspending the cells in 50 mM phosphate buffer, 500 mM NaCl at pH 7.3 (Buffer A) containing EDTA-free protease inhibitor (Roche), lysed in a French Press at 1000 psi, and centrifuged at 8500g for 30 min. The supernatants were loaded onto an affinity column containing chitin beads (New England Biolabs). The apoproteins were cleaved from the intein by incubating overnight at 4 °C with 50 mM 2-mercaptoethanesulfonate (MESNA) in Buffer A. The eluted protein fractions were assayed for purity by sodium dodecyl sulfate-polyacrylamide gel electrophoresis (SDS-PAGE) analysis on an Amersham Biosciences PHAST system using gradient10–15 gel (GE Healthcare). Fractions containing the proteins were collected and then concentrated to about 10 mL in an Amicon Ultra-15 centrifugal filter with a molecular mass cutoff of 5 kDa. The

protein concentrations were determined by Bradford analysis. The concentration as measured by Bradford assay was comparable to that measured at OD<sub>280</sub> using the calculated extinction coefficient of 19,940 M<sup>-1</sup> cm<sup>-1</sup>.<sup>28</sup>

**<sup>15</sup>N-Enriched ScoHM.** <sup>15</sup>N-Enriched ScoHM was grown using in-house made M9 minimal medium containing <sup>15</sup>NH<sub>4</sub>Cl as the source of nitrogen-15. The sterilized M9 minimal medium contained 0.5 g/L <sup>15</sup>NH<sub>4</sub>Cl, 10 mL of 40% glucose, 2 mL of 1 M MgSO<sub>4</sub>, 100  $\mu$ L of IM CaCl<sub>2</sub>, 1 mL of 5% thiamine, 10 mL of 0.1% biotin, 1 mL of 10% ampicillin, 200 mL 5x M9 salts, and 778 mL sterile deionized water. Apo-<sup>15</sup>N-Enriched ScoHM was expressed and purified with modification to the method described previously.<sup>29</sup> In a typical expression experiment, <sup>15</sup>N-enriched ScoHM was grown by inoculating 10 mL of LB-glucose medium with a single colony of cells expressing ScoHM at 37 °C. After 8 h, a 100  $\mu$ L aliquot of LB culture was diluted into 10 mL of N15-enhanced M9 minimal medium and grown overnight at 37 °C. The overnight culture was then transferred into 1 L of N15-enhanced M9 minimal medium and allowed to grow at 37 °C until OD<sub>600</sub> was between 0.5 and 0.9. Expression of <sup>15</sup>N-enriched ScoHM was induced by the addition of 0.5 mM IPTG at 17 °C shaking for 20 h. The cells were harvested by centrifugation in a Sorvall GS-3 rotor at 8000g for 30 min and frozen at -80 °C. The <sup>15</sup>N-enriched ScoHM was purified using the method described above.

**Reconstitution with Cu(II) and Pure <sup>65</sup>Cu(II) Isotope.** Apo-ScoHM and its 5'-Stag ScoHM variant were dialyzed into three buffer changes of 50 mM phosphate buffer at pH 8.0 (buffer B) to remove excess MESNA present in the protein solution. Cu(II) reconstitution was performed by adding at least 3 molar equiv of CuSO<sub>4(aq)</sub> to the apoproteins at room temperature. Excess Cu(II) was removed by dialysis against three changes of metal-free buffer B. Fully reconstituted <sup>65</sup>Cu(II)-ScoHM and <sup>15</sup>N-enriched ScoHM proteins were prepared by adding stoichiometric equivalents of <sup>65</sup>CuCl<sub>2</sub> to the apoproteins. <sup>65</sup>CuCl<sub>2</sub> was prepared from <sup>65</sup>CuO (Oak Ridge) as described previously.<sup>30,31</sup> Cu(II) titration experiments with either natural-abundance Cu or <sup>65</sup>Cu were achieved by adding, incrementally, the required fractional amounts of copper to the protein solutions.

**Reconstitution with Cu(I).** Cu(I) reconstitution of ScoHM protein was performed in an anaerobic chamber to prevent the oxidation and/or disproportionation reaction of Cu(I) under aerobic conditions. To further avoid the presence of oxygen in the protein solution, all buffer solutions used were predegassed by purging with argon in an airtight container for at least 1 h. Degassed solutions were then transferred into the anaerobic chamber. Apo-protein samples were also degassed by dialyzing overnight into degassed 50 mM phosphate buffer at pH 8.0. The sample was reconstituted with Cu(I) by slow infusion of the required molar equivalents of [Cu(I)-(CH<sub>3</sub>CN)<sub>4</sub>]PF<sub>6</sub> dissolved in 100% acetonitrile. After the addition of Cu(I), the reconstituted protein was quickly spun through 3 sets of pre-equilibrated desalting spin columns (Pierce) to remove excess, unbound Cu(I). The immediate use of the desalting spin column prevented ScoHM from precipitation in the presence of excess Cu(I).<sup>32</sup> The concentration of copper bound to the proteins was measured on a Perkin-Elmer Optima 2000 DV inductively coupled plasma optical emission spectrometer (ICPOES). The same reconstitution steps were repeated for the Cu(I) reconstitution of 5'-Stag ScoHM variant. Cu(I)-ScoHM samples were also prepared by treating the Cu(II)-bound forms with a 5-fold excess of ascorbate buffered at the same pH.

**Analysis of ATP7A Membrane Fraction on Blue Native Gels.** HEK293Trex cells were treated with 100  $\mu$ M BCS or 100  $\mu$ M CuCl<sub>2</sub> for 3 h. Cells were then resuspended in 2 mL of the lysis buffer (25 mM imidazole pH 7.4, 250 mM sucrose, 5 mM DTT, 2 mM AEBSEF, and 1 tablet of Roche Complete protease inhibitor cocktail (EDTA-free) per 50 mL buffer). Cells were homogenized in Dounce homogenizer and centrifuged at 500g for 10 min. Supernatant was collected and centrifuged at 20,000g for 45 min to sediment microsomal membranes. Pelleted membranes were solubilized in 50 mM Bis-Tris pH 7.0, 50 mM NaCl, 10% glycerol, 0.5% DDM (v/v) on ice for 1 h and then centrifuged at 20,000g for 10 min. Supernatant (10  $\mu$ g of protein) was analyzed by Blue-Native gel (4–16% Invitrogen

NativePage Novex Bis-Tris Gel, 15 wells) after adding 1 volume of 10x loading buffer (0.5 M aminocaproic acid and 5% Brilliant Blue G250).

The proteins separated on Blue Native gels were transferred to PVDF membrane with transfer buffer of 25 mM Tris and 192 mM glycine at 200 mA for 4 h. Membranes were blocked with 5% milk in PBS at room temperature for 3 h, briefly washed, and incubated with primary antibodies at 1:5000 dilution in 1% milk/PBS in the cold room overnight or at room temperature for 1 h. Secondary antibodies were used at 1:10000 dilution in PBS/Tween. Bands were detected using SuperSignal West PICO Chemiluminescent substrate from Thermo Scientific.

**EPR Spectroscopic Measurements.** Qualitative EPR spectra on ScoHM samples were recorded on a Bruker Elexsys E500 spectrometer equipped with a Bruker ER049X SuperX microwave bridge and an E27H lock-in detector. Spectra were recorded at X-band frequency of 9.4 GHz and at a temperature of 100–120 K, which was maintained by continuous cooling of the cryostat and sample with liquid nitrogen. Data were collected under nonsaturating microwave power conditions, set at 60 db receiver gain, 100 kHz modulation frequency, and modulation amplitude of 4 G. A total of 3 scans, consisting of 2048 points at a sweep time of 167 s were averaged for each data set. The concentrations of paramagnetic copper in the samples were determined by reference of the double integral of the protein samples to Cu(II)-EDTA standard curve of known concentration (200–1000  $\mu\text{M}$ ). High-resolution isotope-dependent spectra for simulation ( $^{15}\text{N}$ -labeled Sco-HM reconstituted with  $^{65}\text{Cu}$ (II)) were recorded at the Illinois EPR Center on a Varian E-122 spectrometer. The samples were run as frozen glasses at  $\sim 110$  K using a continuous nitrogen flow cryostat system. Magnetic fields were calibrated with an NMR gaussmeter. Simulations were carried out using the SIMPIPM program developed at the University of Illinois.<sup>33</sup>

**X-ray Absorption Spectroscopy (XAS), Data Collection, and Analysis.** Cu K-edge data (8.980 keV) data were collected in February 2009, June 2009, and May 2010 at the Stanford Synchrotron Radiation Lightsource. The extended X-ray absorption fine structure (EXAFS) and the X-ray absorption near edge structure (XANES) data were measured on beamline 9-3, operating at 3 GeV with beam currents either between 200 and 160 mA (2010) or between 100 and 80 mA (2009). The beamline was configured with a Si[220] monochromator (crystal orientation  $\varphi = 90^\circ$ ), and a Rhodium (Rh)-coated mirror upstream of the monochromator with a 13 keV (Cu) energy cutoff to reject harmonics. A second Rh mirror downstream of the monochromator was used to focus the beam. Data were collected in fluorescence mode using a liquid nitrogen-cooled, high-count-rate Canberra 100-element (2010) or 30-element (2009) Ge array detector with maximum count rates below 120 Khz. Soller slits with a Z-1 metal oxide (Ni) filter were placed in front of the detector to selectively attenuate the elastic scatter peak. Under these conditions, no dead time corrections were necessary. Energy calibration was achieved by reference to the first inflection point of a copper foil (8980.3 eV) placed between the second and third ionization chamber. Four to six scans of a sample containing only sample buffer (50 mM  $\text{NaPO}_4$ , pH 8.0) were collected, averaged, and subtracted from the averaged data of the protein samples to remove Z-1 (Ni)  $K_\beta$  fluorescence and produce a flat pre-edge baseline. Protein samples (80  $\mu\text{L}$ ) were measured as aqueous glasses (containing  $\geq 20\%$  ethylene glycol) at 10–15 K in a liquid helium cryostat. The number of scans collected for each sample varied from 6 to 10, depending on the concentration of copper in the samples. The scans were collected to  $k = 12.8 \text{ \AA}^{-1}$  at the copper K-edge to avoid possible interference by traces of zinc in the samples.

Data reduction and background subtraction were performed with the program modules of EXAFSPAK.<sup>34</sup> Data from each detector were inspected for glitches, drop-outs before inclusion in the final average. Spectral simulation was carried out by least-squares curve fitting using the program EXCURVE 9.2 as previously described.<sup>7,35,36</sup> The quality of the fits was evaluated by the goodness-of-fit parameter,  $F$ , obtained at the end of the simulation.  $F$ , as defined, is also referred to as the fit index.

$$F^2 = \frac{1}{N} \sum_{i=1}^N k^6 (\text{data}_i - \text{model}_i)^2$$

**Copper Transfer from ScoHM to PHM.** The PHM catalytic core was isolated from the Chinese hamster ovary cell line and purified as described previously.<sup>37,38</sup> To assess copper transfer from ScoHM to PHM, predegassed apo-PHM was added to a reaction vial containing 1 molar equiv (on a per copper basis) of 5'-Stag ScoHM fully loaded with either Cu(I) or Cu(II). The mixture was then incubated at room temperature under strictly anaerobic conditions. After 1 h, 1 mL of the ScoHM-PHM mixture was transferred onto a 1 mL strep-tactin resin column (IBA BioTAGnology) equilibrated with buffer (50 mM  $\text{NaPO}_4$ , 150 mM NaCl, pH 8.0) and incubated for an additional 1 h. Proteins were separated by washing 5 times with 1 column volume of buffer, followed by elution of bound 5'-Stag ScoHM with 2.5 mM desthiobiotin in the same buffer. All wash and elution fractions were collected and analyzed for copper and protein content. The protein content in each of the elution fractions was analyzed by SDS-PAGE. To demonstrate that copper transfer to PHM resulted from the direct interaction of PHM with copper loaded ScoHM, a control experiment was performed in which chelex resin was added to the reaction mixture. In the control experiment, the appropriate amount of chelex resin ( $\sim 0.002$  g) was added to chelate an amount of free Cu(II) equivalent to the total amount of protein-bound copper. After 1 h of gentle agitation of the reaction mixture with a magnetic stirrer, the protein mixture was spun down for 1 min at 3000 rpm. The supernatant solution containing the protein mixture was transferred onto the strep-tactin column and subjected to the procedure described above.

**Determination of PHM Activity after Copper Transfer from ScoHM.** PHM activity was measured by HPLC using dansyl-Tyr-Val-Gly as fluorescent substrate, or by oxygen consumption in an  $\text{O}_2$ -sensitive electrode, as described in detail previously.<sup>39</sup>

## RESULTS

**Binding of Cu(II) to the ScoHM Luminal Loop.** When ScoHM was incubated with an excess of cupric ion, followed by exhaustive dialysis or desalting, it bound  $1.9 \pm 0.2$  molar equiv of Cu(II) per protein. This suggests the presence of two binding sites in the fully loaded complex. EPR and XAS studies were undertaken to determine the coordination environment of each of these sites.

**EPR of Cu(II)-Binding to ScoHM.** Figure 1 shows an EPR titration of ScoHM with increasing amounts of cupric ion. At copper to protein ratios below 1:1, a type 2 EPR spectrum is obtained with well-resolved superhyperfine splittings in the  $g_{\perp}$  region. As the copper to protein ratio is increased above 1, new features appear, accompanied by the loss of superhyperfine structure. The final spectra are at least two-component and confirm that two separate Cu(II) species are present. At the highest copper to protein (2.5:1) the superhyperfine is lost, although the spectrum integrates to 100% Cu(II). This suggests that addition of a second Cu(II) to the loop causes line broadening, perhaps due to dipolar relaxation effects, but that the two copper centers cannot be close enough to cause exchange coupling of their respective spins.

Simulations were carried out on spectra collected from  $^{65}\text{Cu}$ -labeled protein at 1:1 and 2.5:1 copper to protein. At 1:1, good fits (Figure 1b) could be obtained by assuming a single species with  $g_z = 2.254$ ,  $g_x = 2.075$ ,  $g_y = 2.040$ . The superhyperfine splittings in the  $g_{\perp}$  region of the spectrum could be simulated equally well by 2–4 equivalent N ligands. To distinguish between these possibilities higher resolution EPR spectra were collected at 0.45:1 and at 0.9:1 Cu to protein from a sample obtained from cells globally labeled with  $^{15}\text{N}$ , and these are compared with  $^{14}\text{N}$  spectra in Figure 2a. Close inspection

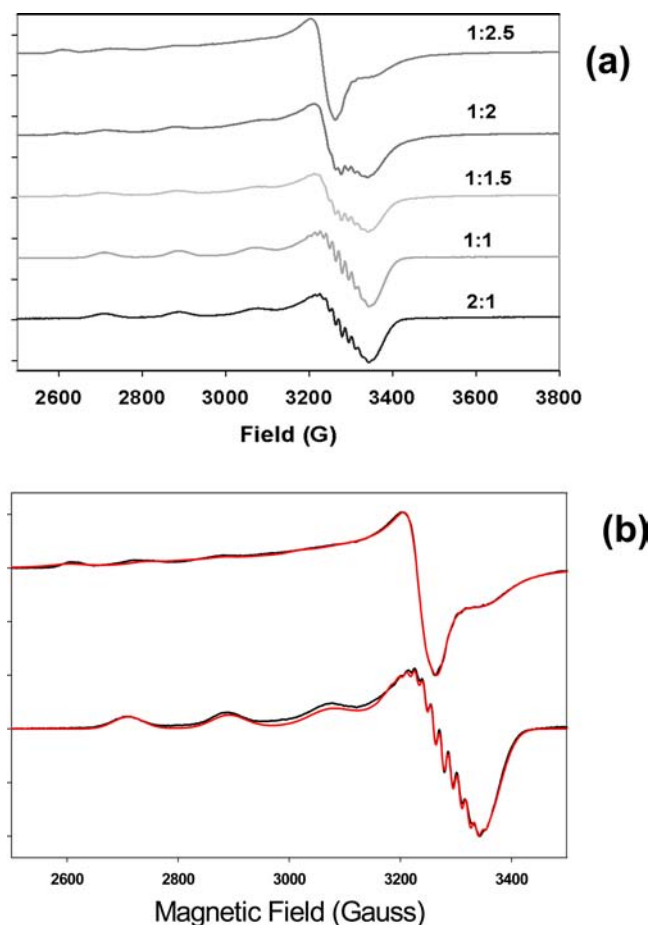


**Figure 1.** (a) EPR titration of apo-ScoHM with Cu(II). Apo-ScoHM was titrated with 0.5 mole equivalents of Cu(II) to generate spectra with protein to Cu(II) ratios as shown. (b) Simulation of ScoHM +Cu(II) EPR spectra. Bottom: 1:1 Protein to Cu(II) as a single component with four equivalent nitrogens  $g_x = 2.075$ ,  $g_y = 2.040$ ,  $g_z = 2.254$ ,  $A_x = -59$ ,  $A_y = -27$ ,  $A_z = -567$  MHz,  $A_x(N) = -28$ ,  $A_y(N) = -42$ ,  $A_z(N) = -24$  MHz, microwave frequency 9.40 GHz, receiver gain 60db, microwave power 2 mW, modulation amplitude 4G,  $T = 100\text{--}120$  K.

reveals differences in the superhyperfine structure on both the low-field  $g_{||}$  line and in the  $g_{\perp}$  region for  $^{15}\text{N}$  and  $^{14}\text{N}$  spectra, respectively. The  $^{15}\text{N}$  spectra (Figure 2b) have 5 superhyperfine low-field lines, while the  $^{14}\text{N}$  spectra (Figure 2c) are less well-resolved but appear to have 9 lines. From these empirical data we predict that the Cu(II) is coordinated to 4 equivalent N ligands where the number of lines  $n$  is equal to  $2nI + 1$ . Simulation of  $^{14}\text{N}$  (Supplementary Figure S1b) and  $^{15}\text{N}$  (Supplementary Figure S1c and d) gives good fits with 4 equivalent N ligands and spin Hamiltonian parameters listed in Supplementary Table S1.

At ratios above 1:1 copper to protein, the spectra broaden eventually losing all superhyperfine splittings at or above 2:1. The  $^{65}\text{Cu}/^{14}\text{N}$  EPR spectrum of this final spectrum was collected under lower resolution and simulated as shown in Figure 1b. The simulations required the presence of two distinct species present at approximately 1:1 ratio both of which differed from that observed at or below 1:1. Spin Hamiltonian parameters are listed in the legend to Figure 1.

**Dimerization of the Luminal Loop and ATP7A.** These data are consistent with the formation of multiple distinct coordination environments for Cu(II) as the copper to protein

ratios increase. At low ratios, a species with 4 equivalent N ligands (most likely imidazole side chains from His residues) predominates. During the titration, this species appears to be almost fully formed at a ratio of 0.5 coppers per protein, and its spectral intensity changes little between 0.5 and 1:1 ratios. Comparison of  $^{15}\text{N}$  spectra at 0.43 and 0.90 equiv Cu(II) per protein are shown in Supplementary Figure S1a. The 0.45 and 0.9 Cu:P spectral simulations differ only in the presence of an additional broad structureless background in the 0.9:1 data, which accounts for the increase in the total cupric content. This suggests a dimeric form, in which Cu(II) is coordinated by two His residues from each of two protein molecules. Attempts to confirm the presence of a dimer using high performance gel filtration were unsuccessful, showing instead only monomeric species (data not shown). However, the dimer is unlikely to survive the gel filtration process if it is held together solely by copper binding and could dissociate under conditions where free cupric ions are no longer in equilibrium with the  $\text{CuL}_2$  species. As additional Cu(II) loads into the protein, two new sites are formed with distinct  $g$  values and unresolved hyperfine and superhyperfine splittings. This behavior suggests that additional Cu loading breaks apart the dimer and causes Cu(II) binding at two distinct sites in each monomer. The loss of hyperfine is consistent with dipolar broadening due to the presence of two spins at an intermediate distance ( $>5$  Å).

The question arises whether the formation of a dimeric species has physiological relevance with respect to copper release into the lumen. This would require ATP7A to be able to form dimeric or oligomeric structures within the membrane. To address this issue we used HEK293 cells that express ATP7A *endogenously*. These cells were treated with either BCS to deplete copper or with extra copper. We then prepared the ATP7A-containing membranes, solubilized protein with a mild detergent (0.5% dodecyldecamaltoside), and examined the ATP7A oligomeric state on the blue native gels under non-denaturing conditions. The data are shown in Figure 2d. It is apparent that ATP7A migrates as two bands: a minor low molecular weight band and the major higher molecular weight band with a size double that of the minor band. Consequently, we conclude that the predominant form of ATP7A even in copper-depleted cells is an oligomer. It should be noted that in the blue native gels the molecular weight markers do not accurately reflect masses of membrane proteins. ATP7B (165 kDa), which is slightly smaller than ATP7A (180 kDa), is shown as a control. Although formally we cannot exclude the presence of higher order oligomers, our current interpretation is that the low ATP7A band represents a monomer, and the higher band represents a dimer.

**Characterization of the Copper Sites by XAS.** Further characterization of 1:1 and 2:1 complexes was carried out by X-ray absorption spectroscopy. Figure 3 compares Fourier transforms and EXAFS spectra for the 1:1 and 2:1 complexes, respectively. The spectra are dominated by an intense peak at  $\sim 2$  Å but have additional satellite peaks at 3 and 4 Å, respectively, which are fingerprints for imidazole ligation. These spectra therefore establish that Cu(II) is bound by His residues from the loop region. Establishing the ratio of His to non-His O/N ligands depends on accurate simulation of the multiple scattering (MS) interactions that lead to the outer-shell satellite peaks and generally is only semiquantitative due to correlations between scattering amplitudes and Debye–Waller terms and the sensitivity of the MS to small differences in orientation of each Cu–His interaction. Notwithstanding these uncertainties,

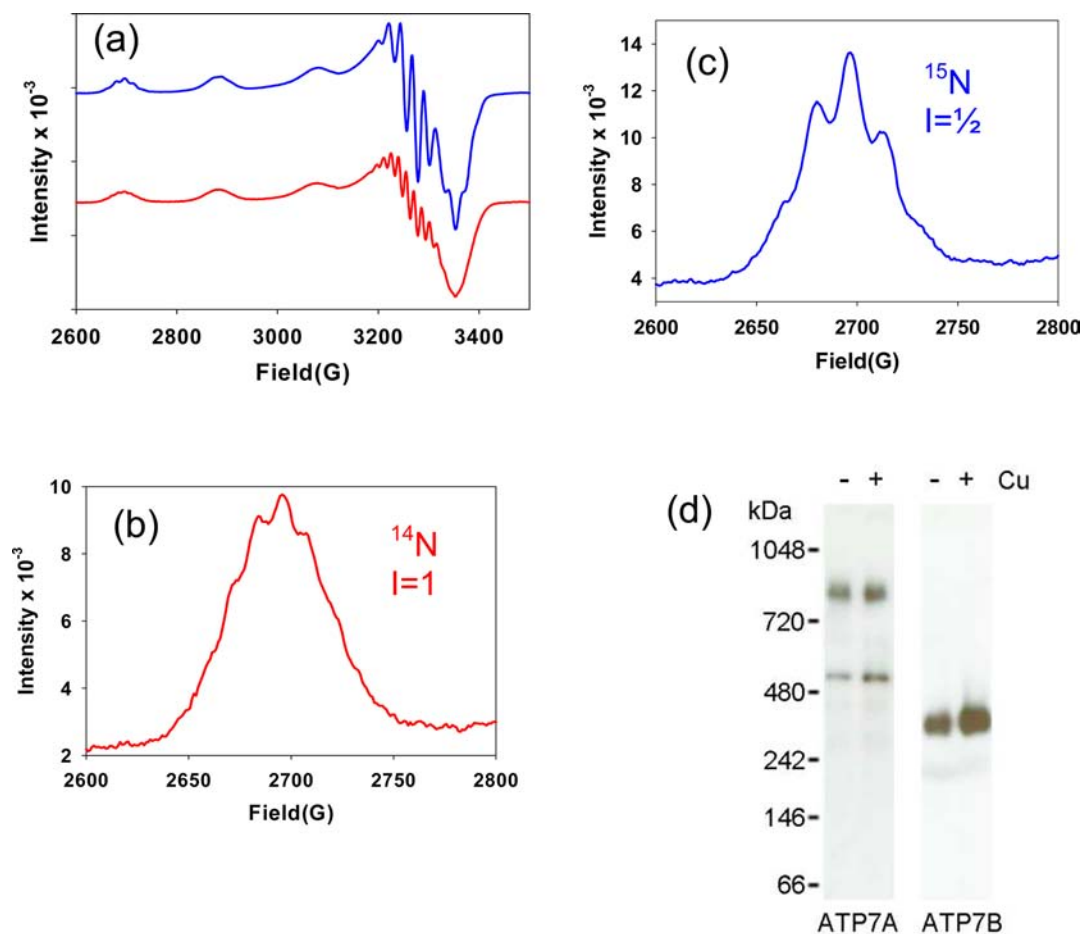


**Figure 2.** (a) Comparison of  $^{14}\text{N}$ - (red) and  $^{15}\text{N}$ - (blue) substituted ScoHM at 1:1 Cu:P. (b) and (c) Low-field hyperfine line expanded to reveal superhyperfine structure for  $^{14}\text{N}$ - and  $^{15}\text{N}$ -substituted proteins respectively. EPR instrumental settings were as listed in the legend to Figure 1. (d) Western blots of ATP7A membranes separated on blue native gels showing the presence of oligomeric forms of ATP7A. ATP7B treated in the same fashion is shown as a control. The following soluble proteins were used as molecular weight markers: 1048 kDa, IgM Pentamer; 720 kDa, Apoferritin Band 1; 480 kDa, Apoferritin Band 2; 242 kDa, B-phycoerythrin; 146 kDa, Lactate Dehydrogenase; 66 kDa, Bovine Serum Albumin.

inspection of the relative amplitudes of the outer-shell transform peaks indicates more His residues coordinated (higher intensity) at 1:1 than at 2:1 ratio (Figure 4). This is confirmed by simulation where the 1:1 ratio sample simulates best with  $4 \pm 1$  His residues, whereas the 2:1 ratio sample simulates best with 2 His + 2 non-His residues, again with  $\sim 25\%$  uncertainty in coordination numbers of each shell. These data therefore support the model developed above in which initial copper loading forms a dimeric structure involving two His residues from each monomer which on further copper addition and breaks apart to form two distinct 4-coordinate monomeric sites with 2 His ligands and additional ligands from either solvent or non-His protein side-chain/main-chain donors. Best-fit simulations of the EXAFS data and the metrical parameters used in the fits are shown in Figure 3 and Table 1, respectively.

In previous work<sup>26</sup> we reported initial data on Cu(I) binding to the ScoHM loop, where different coordination environments were observed at low (1:1) and high (2.5:1) Cu(I) to protein ratios. In the present work, the availability of stable Cu(II) adducts allowed us to use reduction of these Cu(II) species by ascorbate as an alternative route for preparation of the Cu(I)-bound derivatives. Figure 5 shows Fourier transforms and EXAFS spectra for ascorbate-reduced samples at 2:1 (bottom) and 1:1 (top) copper:protein ratios, respectively. The 2:1

samples can be analyzed as a homogeneous 2-coordinate environment with Cu(I) coordinated to two His residues at a characteristically short (1.88 Å) distance. The 1:1 sample on the other hand shows a split first-shell peak due to a mixture of Cu-N and Cu-S coordination, with the best fit simulation predicting two His and one S(Met) ligand at 1.88 and 2.19 Å. Comparison of the absorption edges confirms these assignments, showing an intense 8983 eV feature from the 2-coordinate site in the 2:1 sample and a decreased intensity feature attributable to greater 3-coordinate character in the 1:1 sample (Figure 6). The data suggest that at low copper the dimeric species dissociates on reduction and the Cu(I) redistributes between His and Met residues, whereas at higher Cu:P ratios the 4-coordinate Cu(II)-(His)<sub>2</sub>(O/N)<sub>2</sub> centers reduce cleanly to a pair of 2-coordinate Cu(I)-(His)<sub>2</sub> sites. A likely possibility is that the non-His O/N ligands are solvent molecules that would be expected to dissociate on reduction of the Cu(II) to Cu(I).

**Transfer of Copper to Peptidylglycine Monooxygenase.** We tested the ability of the luminal loop to transfer copper to apo-PHMcc via quantitative measurement of the recovery of enzyme activity using an oxygen-sensitive electrode. We first constructed a ScoHM chimera with a strep-tag fused to the N-terminus. The strep-tag-ScoHM chimera was loaded with Cu(II), mixed with 1 molar equiv (on a per Cu basis) of apo

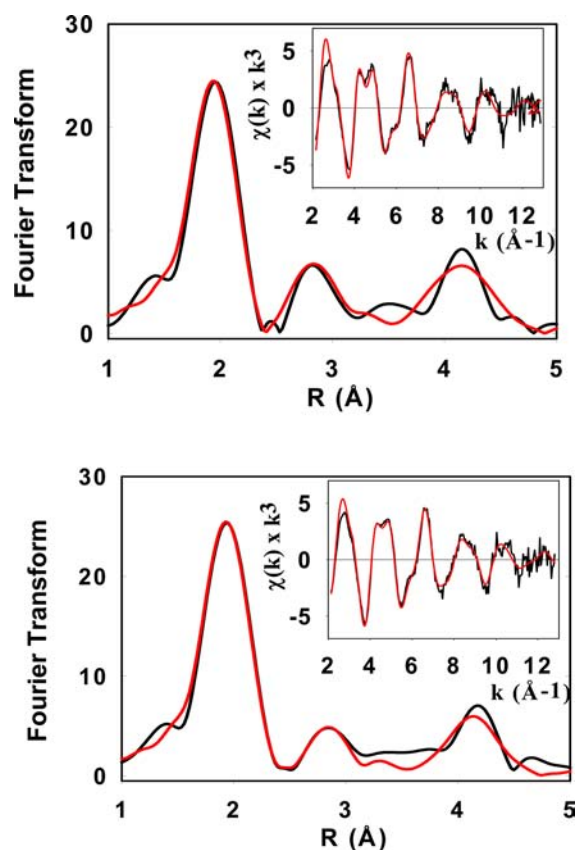


**Figure 3.** Fourier transforms and EXAFS (inserts) of Cu(II) complexes of ScoHM: top 1:1, bottom, 2:1. Black lines represent experimental spectra, red lines represent simulated spectra. Parameters used in the fit are listed in Table 1.

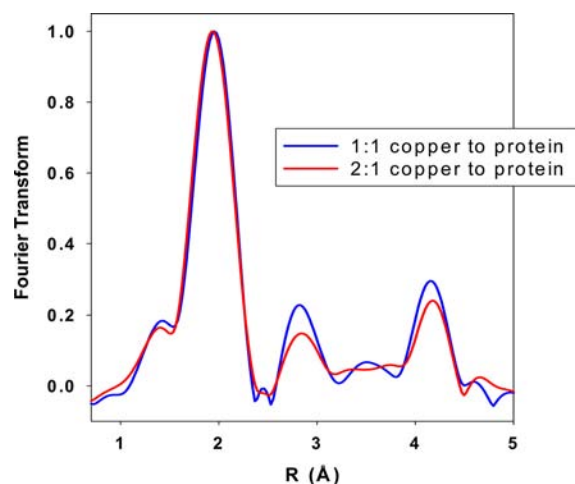


**Figure 4.** Comparison of the Fourier transform intensity for Cu(II) to protein ratios of 1:1 (blue) and 2:1 (red) complexes of ScoHM complexes.

PHMcc, and allowed to react for 1 h. Aliquots of the resulting mixture were added to the assay reagents and catalytic activity was measured by determining the rate of oxygen consumption, at saturating concentrations of N-Ac-YVG and ascorbate. Determining transfer efficiency is complicated by the fact that apo-PHM can be fully reconstituted by aqueous Cu(II) ions *in vitro*. Therefore it is possible that copper could dissociate from ScoHM as aqueous Cu(II) and subsequently react with apo

PHM to form fully metalated enzyme. To guard against this possibility we determined conditions under which added chelex resin would bind free copper quantitatively yet be unable to remove Cu(II) from either PHMcc or ScoHM. It was found that incubation of 300  $\mu$ M PHM or ScoHM with 1 mg of chelex for 4 h resulted in no loss of PHM-bound Cu(II) and less than 10% of ScoHM-bound Cu(II) but removed aqueous Cu(II) quantitatively from solution (Supplementary Figure S2). Rates of oxygen consumption were then determined for PHM reconstituted with ScoHM in the presence and absence of 1 mg chelex, together with negative controls consisting of apo-PHM, and Cu(II)-loaded ScoHM with no PHM, and a positive control consisting of PHM fully reconstituted with aqueous Cu(II), using established procedures. The results (Table 2 and Supplementary Figure S3) show that Cu(II)-loaded ScoHM reconstitutes the enzyme to full activity, yet neither apo-PHM or ScoHM on its own generates activity levels above background. Addition of chelex results in a small decrease ( $\sim$ 20%) in activity suggesting that 80% of copper transfer occurs by direct transfer between the luminal loop and apo PHM.

We also investigated whether copper transfer from the ScoHM generated native forms of PHM as judged by their spectroscopic signatures and by the catalytic activity of the PHM product after separation from the ScoHM copper donor. The proteins were again allowed to react with either Cu(II) or Cu(I) for 1 h and then separated on a strep-tactin affinity column. The untagged PHM did not bind and was collected in the flow-through fraction and buffer washes. The ScoHM fraction carrying the tag bound to the column and was eluted with desthiobiotin. The results of a typical experiment (Figure 7) show that this protocol resulted in a reconstituted PHM protein containing 1.2 Cu's per protein, while the copper content of the ScoHM had decreased from 2 to 0.5 Cu's per ScoHM, indicative of 60–75% transfer. The reconstituted PHM was active as indicated by the HPLC chromatogram in panel c where substrate dansyl-YVG (peak on right) is converted into product dansylYVG-OH (peak in center) as a function of reaction time. For Cu(I) transfer (data not shown), the reconstituted PHM was also analyzed by XAS to ensure correct assembly of the active site. Table S2 (Supporting Information) compares fits to the Cu(I) transfer samples with fully reduced WT PHM.

## DISCUSSION

Maturation of cuproproteins such as tyrosinase, PAM, DBM, and SOD3 involves trafficking of the immature proteins through the TGN into storage vesicles or to the plasma membrane where they react with substrates and accumulate product.<sup>40,41</sup> The maturation process requires metalation with Cu ions and involves interaction with the ATPase ATP7A, which co-locates with the enzyme in the intracellular compartments.<sup>10,11,21</sup> Little is known about the process by which ATP7A hands off copper into the lumen of the secretory pathway (where the soluble domains of the enzymes reside), but available data suggest that specificity is achieved entirely through spatial co-location and does not require the intermediacy of a metallochaperone.<sup>21</sup> Recently we reported on the biochemical and spectroscopic properties of a characteristic His and Met loop of ATP7A that is located between TMs1 and 2 and extends into the luminal space.<sup>26</sup> We showed that this loop bound both Cu(I) and Ag(I) and that mutations in key His or Met residues inhibited the

Table 1. Fits Obtained to the EXAFS of Oxidized and Ascorbate-Reduced Forms of ScoHM

	$F^a$	no. <sup>c</sup>	$R$ (Å) <sup>d</sup>	DW (Å <sup>2</sup> )	no. <sup>c</sup>	$R$ (Å) <sup>d</sup>	DW (Å <sup>2</sup> )	no. <sup>c</sup>	$R$ (Å) <sup>d</sup>	DW (Å <sup>2</sup> )	$-E_0$
Cu(II) ScoHM											
			Cu-N(His) <sup>b</sup>			Cu-O/N			Cu-S		
1:1	0.637	4	1.99	0.015							4.80
1:2	0.357	2	1.93	0.009	2	2.03	0.009				5.04
Cu(I) ScoHM Prepared by Ascorbate Reduction											
			Cu-N(His1) <sup>b</sup>			Cu-O/N			Cu-S		
1:1	0.569	2	1.87	0.016				1	2.19	0.018	-4.3
2:1	0.879	2	1.87	0.011							-1.20

<sup>a</sup> $F$  is a least-squares fitting parameter defined as  $F^2 = (1/N) \sum_{i=1}^N k^6 (\text{data} - \text{model})^2$ . <sup>b</sup>Fits modeled histidine coordination by an imidazole ring, which included single and multiple scattering contributions from the second shell (C2/C5) and third shell (C3/N4) atoms, respectively. The Cu–N–C<sub>x</sub> angles were as follows: Cu–N–C2, 126°; Cu–N–C3, -126°; Cu–N–N4, 163°; Cu–N–C5, -163°. <sup>c</sup>Coordination numbers are generally considered accurate to ±25%. <sup>d</sup>In any one fit, the statistical error in bond lengths is ±0.005 Å. However, when errors due to imperfect background subtraction, phase-shift calculations, and noise in the data are compounded, the actual error is probably closer to ±0.02 Å.

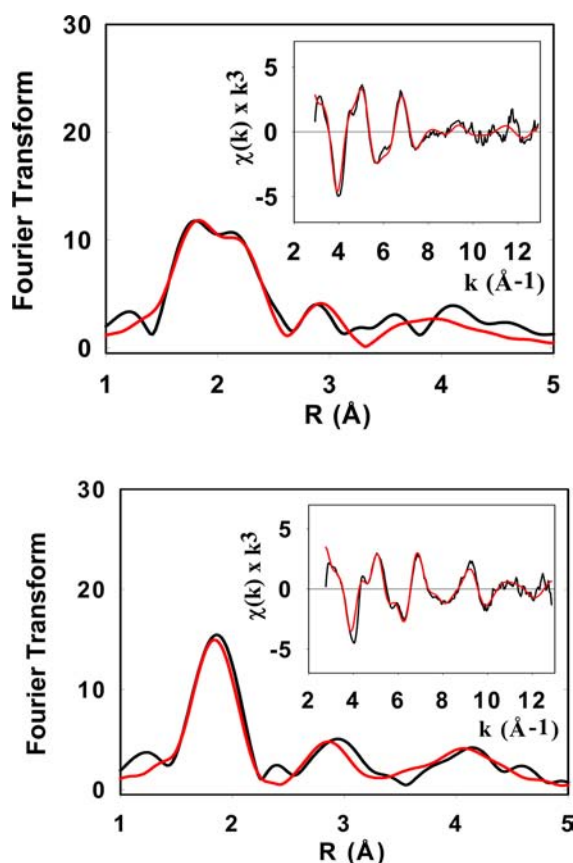


Figure 5. Fourier transforms and EXAFS (inserts) of Cu(I) complexes of ScoHM prepared by ascorbate reduction of their Cu(II) homologues. Top panel Cu(I) to protein 1:1, bottom panel Cu(I) to protein 2:1. Black lines represent experimental spectra, red lines represent simulated spectra. Parameters used in the fit are listed in Table 1.

dephosphorylation step of ATP7A catalysis, suggesting a role in copper release. Because the full-length ATP7A binds copper to each of its six N-terminal subdomains as well as to sites within the membrane and the loop sequence was unstable as an isolated peptide, we created a chimera with a scaffold protein by substituting the loop sequence for the CETIC copper-binding motif of *B. subtilis* Sco, in which all other His and Met residues had been mutated to Ala or Ile. In the present paper we have used XAS and EPR to characterize (a) the species formed when the loop binds Cu(II), (b) the species formed when the Cu(II)-

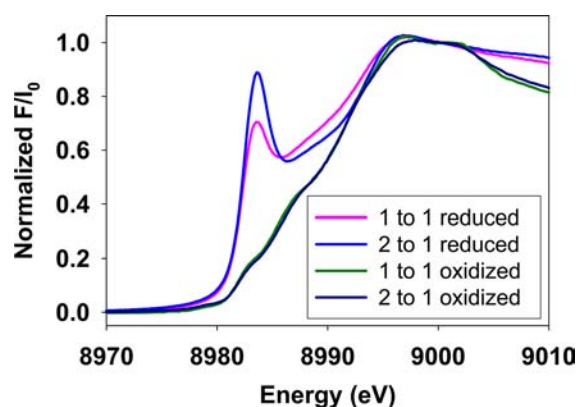


Figure 6. Comparison of XANES for oxidized and reduced forms. Spectra from the bottom are as follows: black trace 2:1 Cu(II) to protein, green trace 1:1 Cu(II) to protein, pink trace 1:1 Cu(I) to protein, blue trace 2:1 Cu(I) to protein.

Table 2. PHM Activity in Samples Reconstituted with Cu(II)-Loaded ScoHM

protein sample	mg of protein	activity (μmol O <sub>2</sub> mg <sup>-1</sup> min <sup>-1</sup> )
Cu(II)-ScoHM	0.0124	0.043
Apo PHM	0.0124	0.234
Cu(II)-PHM <sup>a</sup>	0.0124	3.216
Cu(II)-ScoHM-PHM Mix <sup>b</sup>	0.0124	3.096
Cu(II)-PHM fraction <sup>c</sup>	0.0186	1.830

<sup>a</sup>Positive control composed of a sample of native PHM reconstituted with aqueous Cu(II) to a ratio of 2.0 copper per protein. <sup>b</sup>Mixture of equimolar amounts of apo PHM and Cu(II)-loaded ScoHM. <sup>c</sup>Reconstituted PHM fraction after separation from strep-tagged ScoHM on a streptavidin column.

bound forms are reduced by ascorbate, and (c) the ability of both Cu(II) and Cu(I) forms to transfer copper to the PHM catalytic core.

EPR and EXAFS data of Cu(II)-ScoHM both support a model in which at least two different Cu(II)-binding species form as a function of copper loading. At low Cu, <sup>15</sup>N superhyperfine splittings confirm the presence of 4 equivalent N ligands, whereas at higher Cu to protein ratios species with fewer His residues per Cu predominate. Since the Cu-His<sub>4</sub> species appears to be fully formed at Cu/P ratios below 1, a possible explanation is a dimer formed by one HH doublet from each of two ScoHM molecules. This situation could be an

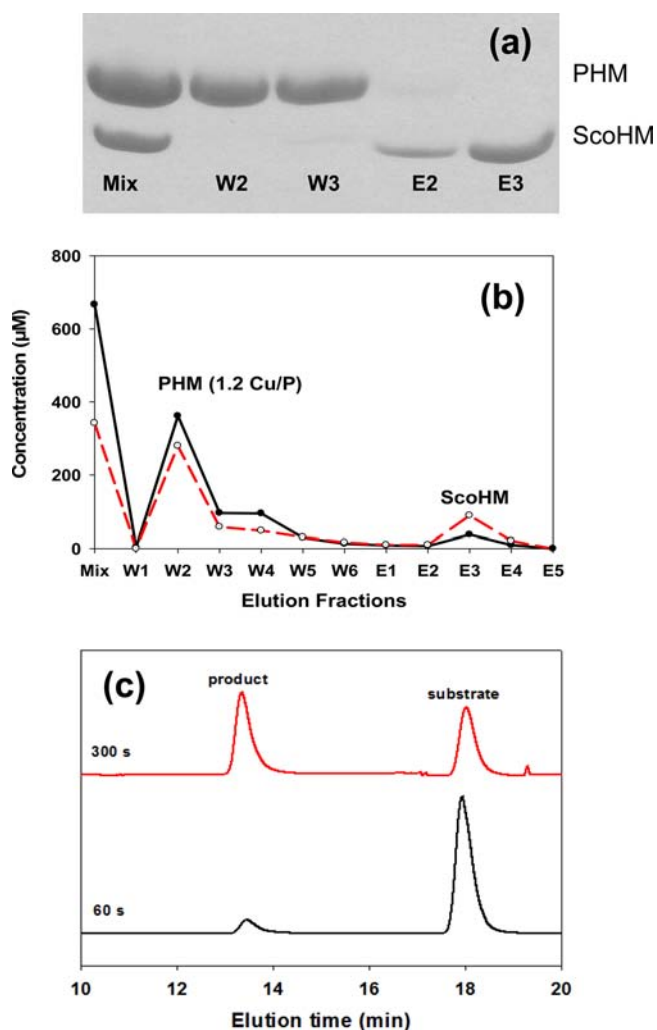


**Figure 7.** Transfer of Cu(II) from Cu(II)-loaded ScoHM to apo-PHM. (a) Separation of proteins on PAGE after mixing and transfer: initial mixture (lane 1), buffer washes (lane 2-3) and the desthiobiotin elution fractions (lane 4-5). (b) HPLC gel permeation chromatography of separated fractions in (a): black traces represent total copper concentration and red traces represent protein concentrations. (c) Conversion of substrate (dansyl-YVG) into product (dansyl-YVG-OH) catalyzed by PHM fraction W2.

artifact of the small size of the scaffold that holds the loop, which would have little relevance to physiological transport if the full length ATP7A existed solely as a monomer in the membrane. However, we have shown using blue-native gels that ATP7A certainly forms higher order oligomers, which are in all probability dimers. Therefore the idea that copper release might involve a transient binding site at the interface of two luminal loop structures from each of two ATP7A molecules is not excluded by our data. Alternatively, it is possible that all four His residues are derived from the two HH pairs in a single molecule. Copper binding to peptides and peptide fragments has been studied in other systems and offers informative comparisons with the ATP7A luminal loop peptide. The HH motif has been shown to bind Cu(II) in a variety of systems that include a fragment of the Alzheimer's amyloidogenic peptide A $\beta$ ,<sup>42</sup> but also in enzymes such as PHM H-site<sup>6</sup> and the Cu<sub>B</sub> center of cytochrome *c* oxidase.<sup>43</sup> However, to our knowledge no case of two pairs of HH motifs binding to Cu(II) has been reported previously.

As the Cu:P ratio increases above 1:1, the mode of binding changes, involving two binding sites each of which appears to have fewer histidine residues. This is reminiscent of Cu(II) binding to the Prion protein, where different Cu(II)-bound species are observed at different ratios.<sup>44–46</sup> At low copper, the octarepeat region, a domain composed of four or more tandem repeats of the motif PHGGGWGQ, binds a single Cu(II) in a square planar environment involving four histidine residues (one from each repeat). At higher Cu(II) to protein ratios, the domain binds four Cu(II) ions with one His, two deprotonated amide nitrogens, and a main-chain carbonyl oxygen as ligands. The amyloidogenic unstructured region of the Prion protein contains an additional two His residues, and both of these have been proposed to bind Cu(II) via the His and three amide N ligands. Binding of Cu(II) by a single His residue and additional amide N donors is also found in the ATCUN (amino terminal Cu and Ni binder)<sup>47</sup> where a His residue occurs at position 3 in the sequence.

The present study has shown that the Cu(II)-bound luminal loop is readily reducible by ascorbate to a Cu(I)-bound form, the coordination of which is also dependent on the degree of copper loading. Reduction of 1:1 Cu(II)/P samples generates a Cu(I)-binding site with both His and Met coordination, whereas reduction of the 2:1 Cu(II)/P sample generates a 2-coordinate Cu(I)His<sub>2</sub> species. These findings are similar to our published data on Cu(I) binding induced by reaction of apoprotein with copper(I) tetrakis-acetonitrile [Cu(I)-(MeCN)<sub>4</sub>]<sup>+</sup> and confirm that multiple conformational states exist for Cu(I) binding as a function of copper loading involving both homogeneous Cu(I)-His<sub>2</sub> and mixed Cu(I)-(His)-(Met) environments. Both of these Cu(I)-binding environments are common for Cu(I). Mixed His/met coordination is found in the transporters/metallochaperones CusF,<sup>48,49</sup> PCu<sub>A</sub>C,<sup>50</sup> PcoC,<sup>51,52</sup> and CopC,<sup>53,54</sup> as well as enzyme active sites such as the catalytic site of PHM,<sup>6</sup> DBM,<sup>8</sup> and TBM.<sup>55</sup> Cu(I)His<sub>2</sub> coordination is also well-documented and appears to be particularly stable. Two independent studies have shown that an HH doublet present in a synthetic fragment of the A $\beta$  Alzheimer's peptide forms a stable linear 2-coordinate complex with Cu(I) that is highly resistant to oxidation by O<sub>2</sub>.<sup>42,56</sup>

The Cu-bound forms of the luminal loop are able to transfer copper in either oxidation state to the cuproprotein acceptor PHM to form fully active enzyme when added to an assay mixture as a 1:1 mixture of fully loaded ScoHM and apo-PHM. Addition of chelex resin in quantities sufficient to bind all of the copper (if present as aqueous Cu(II)) has a minimal effect on the resulting catalytic activity of the reconstituted PHM, suggesting that the transfer occurs via a direct protein–protein interaction, or at least by an “inner-sphere” pathway, and does not involve dissociation of Cu(II) from the donor into the aqueous phase followed by capture by the acceptor protein. Transfer also occurs when the reaction is carried out at higher protein concentrations, and the products separated by affinity chromatography. However, under the latter conditions, the transfer is incomplete, proceeding to approximately 70%. This is not unusual for transfer between chaperone-target pairs where the shallow thermodynamic gradient often leads to an equilibrium distribution of copper over both proteins.<sup>36,57</sup> Analysis of the XAS spectra of the Cu(I) form of the reconstituted PHM product revealed essentially no differences from enzyme fully loaded with 2 Cu, suggesting that the H and M centers of the reconstituted enzyme are both equally

populated, thereby generating active enzyme. As yet we have not been successful in identifying the ligand environment of the copper remaining in the ScoHM. Since both PHM and ScoHM each contain copper centers that are chemically/structurally distinct, the question remains whether there is specificity in the metalation of the H and M centers in PHM by the different copper centers in ScoHM. Additionally, we have not as yet identified any protein–protein complexes, nor have we been able to monitor the kinetics of the transfer although experiments to achieve each of these goals are ongoing. However, despite the fact PHM is easily reconstituted by Cu(II)-aquo ions, it does not accept copper from simple chaperones such as Cu(I)-ATOX1, even though the Cu(I) chelator BCA is able to compete effectively with both proteins in the same concentration range (unpublished data). This emphasizes that interprotein specificity is important and further suggests that kinetic rather than thermodynamic effects are controlling the transfer process.

Our findings have important physiological implications. High levels of ATP7A are present in tissues such as pituitary and cerebral cortex, which also express high levels of PAM.<sup>11</sup> Likewise, tissues of mice with inactivated *atp7a* show reduced levels of amidated peptides but contain normal levels of PAM that is fully active when assayed in the presence of exogenous copper. The inference is that ATP7A is the source of the catalytic copper in vivo.<sup>11</sup> However, copper delivery within the lumen of secretory granules does not appear to rely on specific chaperones.<sup>21</sup> When expressed in yeast, PHM co-locates with the ATP7A homologue CCC2 in the TGN and is fully loaded with copper in an ATX1-dependent fashion. Since yeast does not contain a PHM or DBM homologue and therefore would not be expected to express a PHM-specific transporter, these results mitigate against a requirement for a luminal copper chaperone. Tyrosinase requires ATP7A for activity<sup>12</sup> and is processed via the secretory pathway of melanocytes, where it likewise co-locates with ATP7A.<sup>13</sup>

These and other data<sup>10</sup> underscore the apparent ability of ATP7A to transfer copper directly to vesicular cuproenzymes with different structures and copper coordination. The observation that (when expressed in a scaffold protein) the ATP7A luminal loop is able to bind both Cu(II) and Cu(I) in a variety of different conformations raises the possibility that the loop acts as a dynamic copper donor that can select a copper conformation appropriate for the particular acceptor protein. The apparent ability of ATP7A to oligomerize may be an additional factor imparting selectivity to the process, allowing copper to bind at the interface of two protomeric loop structures, as suggested for the ScoHM chimera at low Cu to protein ratios. In this way selectivity could be achieved entirely through co-location, without the need for unique chaperone-mediated transfer. The ability of the loop to bind copper in both oxidation states may allow it to present copper to the luminal space in an oxidation state appropriate for the redox conditions within the vesicle. PHM and DBM, which are packaged in dense-core synaptic vesicles with an internal pH of 5, require both ascorbate and oxygen for catalytic activity. Whereas the high levels of ascorbate may favor transfer of Cu as Cu(I), the more oxidizing environment of the vesicle and the stability of the cupric forms of these enzymes do not preclude transfer as Cu(II). Tyrosinase, located in melanosomes at pH 7, does not require an external reductant, instead using the catechol product as a reductant. This makes it more likely that the preferred state for transport of copper into the oxidizing

environment of the melanosome could be the Cu(II) form. These conclusions are further supported by studies on model peptides that suggest that sequences containing both Met and His residues are best able to stabilize copper in both oxidation states.<sup>47,58,59</sup> Further work is underway to clarify the mechanism of selectivity in transfer from ATP7A to cuproenzymes.

## ■ ASSOCIATED CONTENT

### 📄 Supporting Information

Three figures describing the simulation of the <sup>15</sup>N EPR spectrum of ScoHM at Cu:P of 1:1, chelex treatment of ScoHM and PHM, and rates of oxygen uptake by ScoHM reconstituted samples; one table of spin Hamiltonian parameters and one table of EXAFS parameters for Cu(I)-PHM prepared by ScoHM transfer. This material is available free of charge via the Internet at <http://pubs.acs.org>.

## ■ AUTHOR INFORMATION

### Corresponding Author

[ninian@comcast.net](mailto:ninian@comcast.net)

### Present Address

<sup>§</sup>Bioscience Division, Los Alamos National Laboratory, Los Alamos, New Mexico 87545, USA.

### Notes

The authors declare no competing financial interest.

## ■ ACKNOWLEDGMENTS

This work was funded by grants from the National Institutes of Health P01GM01067166 (S.L.) and R01 NS27583 (N.J.B.). We gratefully acknowledge the use of facilities at the Stanford Synchrotron Radiation Lightsource, which is supported by the National Institutes of Health Biomedical Research and Technology Program Division of Research Resources and by the U.S. Department of Energy Office of Biological and Environmental Research.

## ■ REFERENCES

- (1) Prigge, S. T.; Mains, R. E.; Eipper, B. A.; Amzel, L. M. *Cell. Mol. Life Sci.* **2000**, *57*, 1236–1259.
- (2) Klinman, J. P. *J. Biol. Chem.* **2006**, *281*, 3013–3016.
- (3) Rosenzweig, A. C.; Sazinsky, M. H. *Curr. Opin. Struct. Biol.* **2006**, *16*, 729–735.
- (4) Antonyuk, S. V.; Strange, R. W.; Marklund, S. L.; Hasnain, S. S. *J. Mol. Biol.* **2009**, *388*, 310–326.
- (5) Prigge, S. T.; Kolhekar, A. S.; Eipper, B. A.; Mains, R. E.; Amzel, L. M. *Nat. Struct. Biol.* **1999**, *6*, 976–983.
- (6) Prigge, S. T.; Kolhekar, A. S.; Eipper, B. A.; Mains, R. E.; Amzel, L. M. *Science* **1997**, *278*, 1300–1305.
- (7) Blackburn, N. J.; Rhames, F. C.; Ralle, M.; Jaron, S. *J. Biol. Inorg. Chem.* **2000**, *5*, 341–353.
- (8) Blackburn, N. J.; Hasnain, S. S.; Pettingill, T. M.; Strange, R. W. *J. Biol. Chem.* **1991**, *266*, 23120–23127.
- (9) Matoba, Y.; Kumagai, T.; Yamamoto, A.; Yoshitsu, H.; Sugiyama, M. *J. Biol. Chem.* **2006**, *281*, 8981–8990.
- (10) Qin, Z.; Itoh, S.; Jeney, V.; Ushio-Fukai, M.; Fukui, T. *FASEB J.* **2006**, *20*, 334–336.
- (11) Steveson, T. C.; Ciccotosto, G. D.; Ma, X.-M.; Mueller, G. P.; Mains, R. E.; Eipper, B. A. *Endocrinology* **2003**, *144*, 188–200.
- (12) Petris, M. J.; Strausak, D.; Mercer, J. F. *Hum. Mol. Genet.* **2000**, *9*, 2845–2851.
- (13) Setty, S. R.; Tenza, D.; Sviderskaya, E. V.; Bennett, D. C.; Raposo, G.; Marks, M. S. *Nature* **2008**, *454*, 1142–1146.

- (14) Lutsenko, S.; Barnes, N. L.; Barteel, M. Y.; Dmitriev, O. Y. *Physiol. Rev.* **2007**, *87*, 1011–1046.
- (15) Gourdon, P.; Liu, X. Y.; Skjorringe, T.; Morth, J. P.; Moller, L. B.; Pedersen, B. P.; Nissen, P. *Nature* **2011**, *475*, 59–64.
- (16) Lutsenko, S.; LeShane, E. S.; Shinde, U. *Arch. Biochem. Biophys.* **2007**, *463*, 134–148.
- (17) Barteel, M. Y.; Lutsenko, S. *Biomaterials* **2007**, *20*, 627–637.
- (18) Lutsenko, S. *Curr. Opin. Chem. Biol.* **2010**, *14*, 211–217.
- (19) Boal, A. K.; Rosenzweig, A. C. *Chem. Rev.* **2009**, *109*, 4760–4779.
- (20) Kim, B. E.; Nevitt, T.; Thiele, D. J. *Nat. Chem. Biol.* **2008**, *4*, 176–185.
- (21) El Meskini, R.; Culotta, V. C.; Mains, R. E.; Eipper, B. A. *J. Biol. Chem.* **2003**, *278*, 12278–12284.
- (22) Kim, E. H.; Rensing, C.; McEvoy, M. M. *Nat. Prod. Rep.* **2010**, *27*, 711–719.
- (23) Davis, A. V.; O'Halloran, T. V. *Nat. Chem. Biol.* **2008**, *4*, 148–151.
- (24) Long, F.; Su, C. C.; Zimmermann, M. T.; Boyken, S. E.; Rajashankar, K. R.; Jernigan, R. L.; Yu, E. W. *Nature* **2010**, *467*, 484–488.
- (25) De Feo, C. J.; Aller, S. G.; Siluvai, G. S.; Blackburn, N. J.; Unger, V. M. *Proc. Natl. Acad. Sci. U.S.A.* **2009**, *106*, 4237–4242.
- (26) Barry, A. N.; Otoikhian, A.; Bhatt, S.; Shinde, U.; Tsivkovskii, R.; Blackburn, N. J.; Lutsenko, S. *J. Biol. Chem.* **2011**, *286*, 26585–26594.
- (27) Andruzzi, L.; Nakano, M.; Nilges, M. J.; Blackburn, N. J. *J. Am. Chem. Soc.* **2005**, *127*, 16548–16558.
- (28) Gill, S. C.; von Hippel, P. H. *Anal. Biochem.* **1989**, *182*, 319–326.
- (29) Yan, Z.; Caldwell, G. W.; McDonell, P. A. *Biochem. Biophys. Res. Commun.* **1999**, *262*, 793–800.
- (30) Siluvai, G. S.; Mayfield, M.; Nilges, M. J.; DeBeer George, S.; Blackburn, N. J. *J. Am. Chem. Soc.* **2010**, *132*, 5215–5226.
- (31) Siluvai, G. S.; Nakano, M.; Mayfield, M.; Nilges, M. J.; Blackburn, N. J. *Biochemistry* **2009**, *48*, 12133–12144.
- (32) Yatsunyk, L. A.; Rosenzweig, A. C. *J. Biol. Chem.* **2007**, *282*, 8622–8631.
- (33) Nilges, M. J. Illinois EPR Research Center (IERC), University of Illinois, Urbana-Champaign, 1979.
- (34) George, G. N. Stanford Synchrotron Radiation Laboratory, Menlo Park, CA, 1995.
- (35) Ralle, M.; Lutsenko, S.; Blackburn, N. J. *J. Biol. Chem.* **2003**, *278*, 23163–23170.
- (36) Bagai, L.; Rensing, C.; Blackburn, N. J.; McEvoy, M. M. *Biochemistry* **2008**, *47*, 11408–11414.
- (37) Bauman, A. T.; Jaron, S.; Yukl, E. T.; Burchfiel, J. R.; Blackburn, N. *Biochemistry* **2006**, *45*, 11140–11150.
- (38) Bauman, A. T.; Ralle, M.; Blackburn, N. *Protein Expression Purif.* **2007**, *51*, 34–38.
- (39) Bauman, A. T.; Broers, B. A.; Kline, C. D.; Blackburn, N. J. *Biochemistry* **2011**, *50*, 10819–10828.
- (40) Milgram, S. L.; Johnson, R. C.; Mains, R. E. *J. Cell Biol.* **1992**, *117*, 717–728.
- (41) Sobota, J. A.; Ferraro, F.; Back, N.; Eipper, B. A.; Mains, R. E. *Mol. Biol. Cell* **2006**, *17*, 5038–5052.
- (42) Shearer, J.; Szalai, V. A. *J. Am. Chem. Soc.* **2008**, *130*, 17826–17835.
- (43) Tiefenbrunn, T.; Liu, W.; Chen, Y.; Katritch, V.; Stout, C. D.; Fee, J. A.; Cherezov, V. *PLoS One* **2011**, *6*, e22348.
- (44) Viles, J. H.; Klewpatinond, M.; Nadal, R. C. *Biochem. Soc. Trans.* **2008**, *36*, 1288–1292.
- (45) Klewpatinond, M.; Davies, P.; Bowen, S.; Brown, D. R.; Viles, J. H. *J. Biol. Chem.* **2008**, *283*, 1870–1881.
- (46) Chattopadhyay, M.; Walter, E. D.; Newell, D. J.; Jackson, P. J.; Aronoff-Spencer, E.; Peisach, J.; Gerfen, G. J.; Bennett, B.; Antholine, W. E.; Millhauser, G. L. *J. Am. Chem. Soc.* **2005**, *127*, 12647–12656.
- (47) Haas, K. L.; Putterman, A. B.; White, D. R.; Thiele, D. J.; Franz, K. J. *J. Am. Chem. Soc.* **2011**, *133*, 4427–4437.
- (48) Xue, Y.; Davis, A. V.; Balakrishnan, G.; Stasser, J. P.; Staehlin, B. M.; Focia, P.; Spiro, T. G.; Penner-Hahn, J. E.; O'Halloran, T. V. *Nat. Chem. Biol.* **2008**, *4*, 107–109.
- (49) Loftin, I. R.; Franke, S.; Blackburn, N. J.; McEvoy, M. M. *Protein Sci.* **2007**, *16*, 2287–2293.
- (50) Abriata, L. A.; Banci, L.; Bertini, I.; Ciofi-Baffoni, S.; Gkazonis, P.; Spyroulias, G. A.; Vila, A. J.; Wang, S. *Nat. Chem. Biol.* **2008**, *4*, 599–601.
- (51) Wernimont, A. K.; Huffman, D. L.; Finney, L. A.; Demeler, B.; O'Halloran, T. V.; Rosenzweig, A. C. *J. Biol. Inorg. Chem.* **2003**, *8*, 185–194.
- (52) Peariso, K.; Huffman, D. L.; Penner-Hahn, J. E.; O'Halloran, T. V. *J. Am. Chem. Soc.* **2003**, *125*, 342–343.
- (53) Zhang, L.; Koay, M.; Maher, M. J.; Xiao, Z.; Wedd, A. G. *J. Am. Chem. Soc.* **2006**, *128*, 5834–5850.
- (54) Arnesano, F.; Banci, L.; Bertini, I.; Thompsett, A. R. *Structure* **2002**, *10*, 1337–1347.
- (55) Hess, C. R.; Klinman, J. P.; Blackburn, N. J. *J. Biol. Inorg. Chem.* **2010**, *15*, 1195–1207.
- (56) Himes, R. A.; Park, G. Y.; Siluvai, G. S.; Blackburn, N. J.; Karlin, K. D. *Angew. Chem., Int. Ed.* **2008**, *47*, 9084–9087.
- (57) Huffman, D. L.; O'Halloran, T. V. *J. Biol. Chem.* **2000**, *275*, 18611–18614.
- (58) Rubino, J. T.; Riggs-Gelasco, P.; Franz, K. J. *J. Biol. Inorg. Chem.* **2010**, *15*, 1033–1049.
- (59) Jiang, J.; Nadas, I. A.; Kim, M. A.; Franz, K. J. *Inorg. Chem.* **2005**, *44*, 9787–9794.